Available online at www.sciencedirect.com
SCIENCE DIRECT®
Biochimica et Biophysica Acta 1698 (2004) 239–250
BIOCHIMICA ET BIOPHYSICA ACTA
BBA
www.bba-direct.com

Structure–activity relationships for the β-hairpin cationic antimicrobial peptide polyphemusin I☆,☆☆

Jon-Paul S. Powers, Annett Rozek, Robert E.W. Hancock*

Department of Microbiology and Immunology, University of British Columbia, #300-6174 University Boulevard, Vancouver, British Columbia, V6T 1Z3, Canada

Received 9 October 2003; received in revised form 1 December 2003; accepted 10 December 2003

Available online 5 February 2004

Abstract

The solution structure of polyphemusin I was determined using ^{1}H-NMR spectroscopy. Polyphemusin I was found to be an amphipathic, β-hairpin connected by a type I′ β-turn. The 17 low-energy structures aligned very well over the β-sheet region while both termini were poorly defined due in part to a hinge-like region centred in the molecule about arginine residues 6 and 16. Conversely, a linear analogue, PM1-S, with all cysteines simultaneously replaced with serine was found to be dynamic in nature, and a lack of medium and long-range NOEs indicated that this molecule displayed no favoured conformation. Circular dichroism (CD) spectroscopy confirmed that in solution, 50% trifluoroethanol (TFE) and in the presence of liposomes, PM1-S remained unstructured. The antimicrobial activity of PM1-S was found to be 4- to 16-fold less than that of polyphemusin I and corresponded with a 4-fold reduction in bacterial membrane depolarization. Both peptides were able to associate with lipid bilayers in a similar fashion; however, PM1-S was completely unable to translocate model membranes while polyphemusin I retained this activity. It was concluded that the disulfide-constrained, β-sheet structure of polyphemusin I is required for maximum antimicrobial activity. Disruption of this structure results in reduced antimicrobial activity and completely abolishes membrane translocation indicating that the linear PM1-S acts through a different antimicrobial mechanism.

Keywords: Antimicrobial peptide; Polyphemusin I; Nuclear magnetic resonance; β-Sheet

1. Introduction

The invertebrate hemolymph has been found to contain a variety of substances that act to protect the animal from invading microorganisms [1]. Included in these substances are cationic antimicrobial peptides. Of interest are two families of β-sheet peptides isolated from horseshoe crabs; the tachyplesins, from the Japanese horseshoe crab *Tachypleus tridentatus*, and the polyphemusins, from the American horseshoe crab *Limulus polyphemus* [2]. These peptides are 17–18 amino acid residues in length, contain two disulfide bonds and have an amidated C-terminal arginine [1]. Both families of peptides possess antibacterial activity, inhibiting the growth of both Gram-positive and Gram-negative species, and fungi [1], in addition to an ability to prevent the replication of enveloped viruses such as influenza A and HIV [3].

The tachyplesins are particularly well characterized. The structure of tachyplesin I has been determined by nuclear magnetic resonance (NMR) spectroscopy and was found to consist of an anti-parallel β-sheet (residues 3–8 and 11–16), constrained by two disulfide bonds, connected by a β-turn (residues 8–11) [4]. Due to their high sequence similarity (Tachyplesin I: **K**WCFRVCYRG**I**CYR**R**CR-NH_2; Polyphe-

Abbreviations: CD, circular dichroism; D_2O, deuterium oxide; MIC, minimal inhibitory concentration; MHC, minimal haemolytic concentration; NMR, nuclear magnetic resonance; NOESY, nuclear Overhauser effect spectroscopy; NOE, nuclear Overhauser enhancement; TOCSY, total correlated spectroscopy; DQF-COSY, double quantum-filtered correlated spectroscopy; POPC, 1-palmitoyl-2-oleoyl-*sn*-glycero-3-phosphocholine; POPG, 1-palmitoyl-2-oleoyl-*sn*-glycero-3-phosphoglycerol; Tris, tris(hydroxyethyl) amino methane; pH*, pH in D_2O; TFE, trifluoroethanol; $diSC_35$, 3,3-dipropylthiacarbocyanine; LPS, lipopolysaccharide

☆ The structures of polyphemusin I have been deposited at the PDB (http://www.rcsb.org/pdb/) accession code: 1RKK.

The proton chemical shifts of polyphemusin I have been deposited at the BMRB (http://www.bmrb.wisc.edu/) accession code: BMRB-6020.

☆☆Supplementary data associated with this article can be found, in the online version, at doi:10.1016/j.bbapap.2003.12.009.

* Corresponding author. Tel.: +1-604-822-2682; fax: +1-604-822-6041.

E-mail address: bob@cmdr.ubc.ca (R.E.W. Hancock).

1570-9639/$ - see front matter © 2004 Elsevier B.V. All rights reserved.
doi:10.1016/j.bbapap.2003.12.009

musin I: **RR**WCFRVCYRG**F**CYR**K**CR-NH_2, where the differences are indicated in bold), the structures of the polyphemusins have been assumed to be virtually identical to that of tachyplesin I. Indeed the structure of a synthetic polyphemusin variant, T22, was determined by NMR spectroscopy and the secondary structure was found to be related to that of tachyplesin I [3].

Although the structures of some cationic antimicrobial peptides have been determined, their mechanism of action remains controversial. The earliest proposed mechanism involved the interaction of the peptide with the bacterial membrane, insertion and aggregation to form small pores [5]. This was believed to lead to membrane depolarization and death of the microorganism. Recent studies have shown that this may not always be the case, as certain antimicrobial peptides (such as bactenecin and indolicidin) do not cause permanent membrane depolarization [6]. It has been proposed that peptides acting in this manner translocate the cytoplasmic membrane and interact with DNA, RNA or protein synthesis [7,8]. Indeed, DNA and RNA binding has been demonstrated in vitro [9,10] and other studies have demonstrated the inhibition of macromolecular synthesis after treatment with sub-lethal peptide concentrations [11,12].

The role of disulfide bonds in peptide activity has been previously investigated. Linear forms of human α-defensin HNP-1 are completely inactive [13]. In contrast, the chemotactic activity of human β-defensin 3 requires proper disulfide formation while antimicrobial activity does not, and linear analogues possess similar activity with the parent peptides [14]. Conversely, the disulfide bond which forms the loop of bovine bactenecin is required for activity against Gram-negative organisms and is thought to play a role in outer membrane permeabilization [15]. Evidence suggests that linear bactenecin can still adopt a secondary structure upon interaction with membranes. Thus, the role of disulfide bonds in antimicrobial activity seems to vary between peptides as opposed to playing a general role. One possibility is that such a role depends on the ability of linear peptides to form defined amphipathic structures upon membrane contact.

Specific disulfide studies focusing on tachyplesin I have indicated that, in minimal inhibitory concentration (MIC) studies with *Escherichia coli*, linear analogues display a reduced activity with the exception of peptides linearized by the substitution with aromatic amino acids [16]. Structural characterization of these aromatic substituted peptides have revealed that, in the case of tyrosine-substituted analogues, aromatic ring stacking serves to stabilize the β-hairpin structure in solution similar to that of a disulfide bond [17]. These findings suggest that the aromatic substituted "linear" analogues possess similar β-hairpin structure to the parent peptide and thus may account for the similar antimicrobial activity.

In an effort to further explore and define the role that disulfide bonds and β-hairpin structures play in the antimicrobial activity of these peptides, a structure–activity study was undertaken. The peptide polyphemusin I was chosen as a model and an analogue (PM1-S) was synthesized with all four cysteine residues simultaneously substituted with serine. Serine was chosen because in all previous experiments involving linear analogues of tachyplesin, serine analogues were not chosen. In addition, serine is similar in both structure and chemistry to cysteine without the corresponding disulfide bonding ability. To provide a basis for future structure–activity relationship studies of the polyphemusins, the three-dimensional structure of polyphemusin I was determined by ^{1}H-NMR and the structure and antimicrobial activities of the linear analogue were then compared with those of the parent peptide.

2. Materials and methods

2.1. Strains and reagents

The bacterial strains used for the antimicrobial activity assays included *E. coli* UB1005 (F^-, *nal*A37, *met*B1) and its outer membrane altered mutant DC2 [18], a wild-type *Salmonella typhimurium* (*S. typhimurium*) and its defensin-sensitive mutant [19], wild-type *Pseudomonas aeruginosa* (*P. aeruginosa*) K799 and its antibiotic-sensitive mutant Z61 [20], *Enterococcus faecalis* (*E. faecalis*) ATCC29212, methicillin-resistant *Staphylococcus aureus* (*S. aureus*) SAP0017, and a clinical isolate of *Staphylococcus epidermidis* (*S. epidermidis*) obtained from Dr. D. Speert (Department of Medicine, University of British Columbia). Antifungal activity was tested using a lab isolate of *Candida albicans* (*C. albicans*) obtained from Dr. B. Dill (Department of Microbiology and Immunology, University of British Columbia). All strains were grown in Mueller Hinton (MH) broth (Difco Laboratories, Detroit, MI) at 37 °C unless otherwise noted. All lipids were purchased from Avanti Polar Lipids Inc. (Alabaster, AL). The fluorescent dye, $diSC_35$, was purchased from Molecular Probes (Eugene, OR). The enzyme α-chymotrypsin and trypsin/chymotrypsin inhibitor were purchased from Sigma (St. Louis, MO).

2.2. Peptide synthesis

Both polyphemusin I (PM1, RRWC^{a}FRVC^{b}YRGFC-^{bYRKCa}R-NH_2, where superscript letters define the disul-

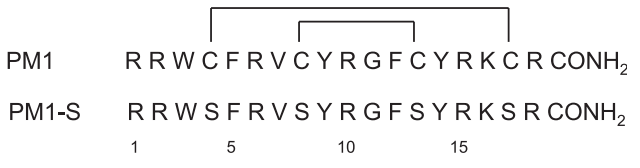

Fig. 1. Primary structures of polyphemusin I (PM1) and its serine-substituted, linear derivative PM1-S. Disulfide linkages in PM1 are shown as solid lines.

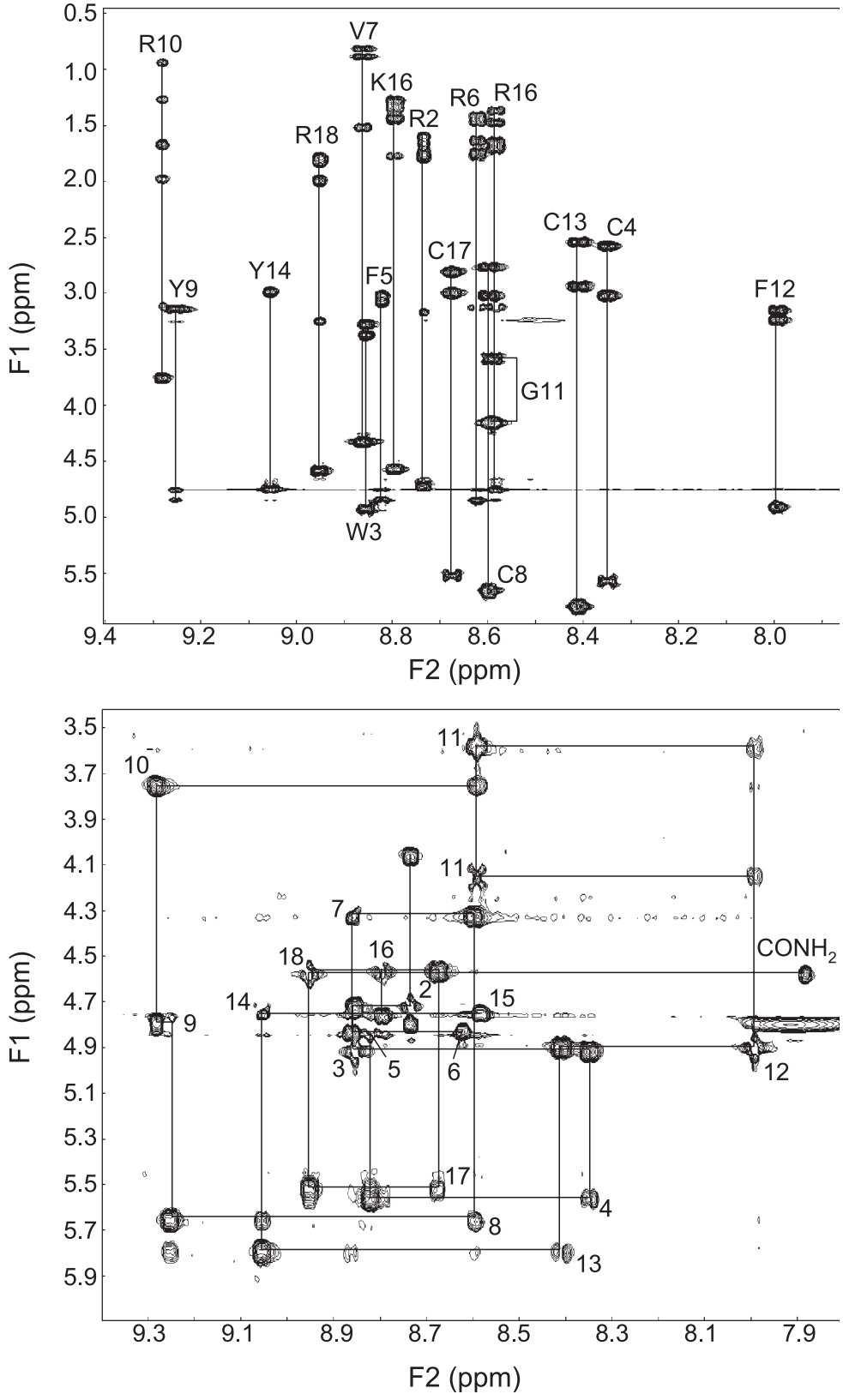

Fig. 2. ^{1}H-NMR spectra of polyphemusin I (PM1). (A) Fingerprint region of the TOCSY spectra of PM1 recorded in H_2O/D_2O (9:1) at 27 °C, pH 4.0. The amino acid spin systems are indicated by one letter code and residue number. (B) NOESY spectra of PM1 recorded in H_2O/D_2O (9:1) at 27 °C, pH 4.0 and a mixing time of 150 ms. The α-amide region is shown and the sequential backbone assignments are connected. For clarity only the intra-residue α-amide crosspeaks are labelled according to residue number.

fide-connected cysteine residues) and the serine-substituted peptide (PM1-S, RRWSFRVSYRGFSYRKSR-NH_2) were synthesized by Fmoc solid-phase peptide synthesis using a model 432A peptide synthesizer (Applied Biosystems, Inc.) at the University of British Columbia Nucleic Acid/Protein service facility. PM1 was then oxidized using a Tris-DMSO-2-propanol solution (100 mM Tris–HCl, 25% DMSO, 10% 2-propanol, pH 7.5) for 24 h at room temperature with constant nutating to promote disulfide bond formation [21]. The correctly folded PM1 was then purified by reverse-phase chromatography using a model LKB FPLC (Amersham Pharmacia). Correct disulfide bond formation (between cysteine residues 4–17 and 8–13) of the purified peptide was confirmed by MALDI mass spectrometry through an observed four mass unit difference between the reduced and oxidized forms of PM1 (data not shown) and further verified through the observation of long-range NOEs in the NOESY spectra of PM1. For clarity, the primary structures and disulfide connectivity of the synthesized peptides PM1 and PM1-S are shown in Fig. 1.

2.3. NMR spectroscopy

Peptides were dissolved in H_2O/D_2O (9:1) at a concentration of 2 mM, pH 4.0. All NMR spectra were recorded at 27 °C on a Varian Inova 600 NMR spectrometer operating at a ^1H frequency of 599.76 MHz. Double quantum-filtered correlated spectroscopy (DQF-COSY) [22], total correlated spectroscopy (TOCSY) [23] and the nuclear Overhauser effect spectroscopy (NOESY) [24] spectra were obtained using standard techniques. Water suppression was achieved using the WATERGATE technique [25,26] or by presaturation. Spectra were collected with 512 data points in F1, 2048 data points in F2. TOCSY spectra were acquired using the Malcolm Levitt (MLEV)-17 pulse sequence [27] at a spin-lock time of 20 ms. NOESY spectra were recorded with a mixing time of 150 ms. The NMR data were processed with NMRPIPE [28].

2.4. NOE data analysis and structure calculation

All NMR spectra were analyzed using NMRView version 5.0.3 [29]. Nuclear Overhauser enhancement (NOE) crosspeaks were assigned and integrated. The NOE volumes were converted to distances and calibrated using intra-residue H^N-Hα crosspeaks and the mean distance of 2.8 Å determined by Hyberts et al. [30]. The distances were then converted into distance restraints by calculating upper and lower distance bounds using the equations of Hyberts et al. [30]. Pseudoatom restraints were corrected as previously described [31] by adding 1 and 1.5 Å to the upper distance bound of unresolved methylene and methyl protons, respectively, and resolved methylene protons were float-corrected by adding 1.7 Å to the upper distance bound. Structure calculations were performed using Xplor-NIH version 2.9.0 [32]. One hundred structures were generated by the DGSA protocol and further refined. The refinement consisted of simulated annealing, decreasing the temperature from 310 to 10 K over 50,000 steps. Forty-seven polyphemusin I structures were calculated with no NOE violations >0.2 Å and the 17 lowest energy conformers with final energies <25 kcal mol^{-1} were selected for presentation. Structural analysis and visualization were performed using Procheck [33,34] and MOLMOL [35].

2.5. Circular dichroism (CD) spectroscopy

CD spectra were recorded on a model J-810 spectropolarimeter (Jasco) using a quartz cell with a 1 mm path

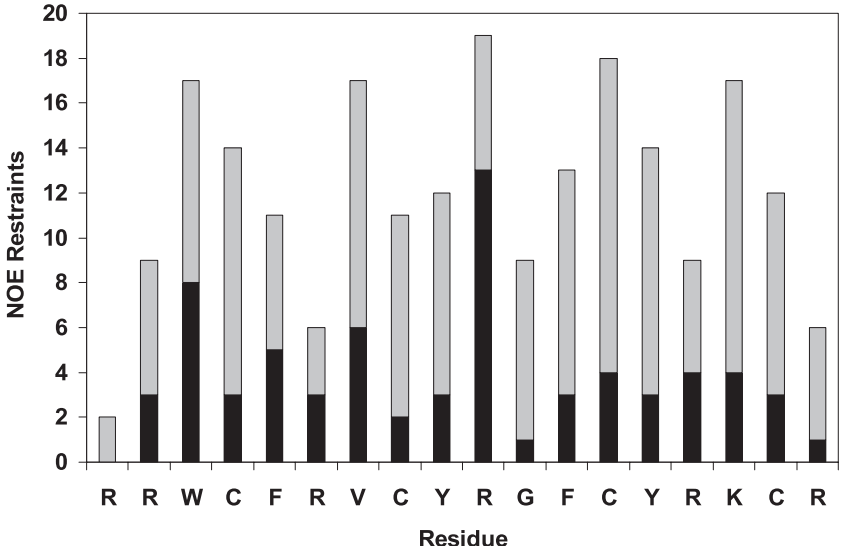

Fig. 3. Number of NOE restraints per residue used during structure calculation of polyphemusin I. Intra-residue and inter-residue restraints are indicated as black and grey bars, respectively.

length. Spectra were measured at room temperature between 190 and 250 nm at a scan speed of 10 nm/min and a total of 10 scans per sample. Spectra were recorded at a peptide concentration of 100 μg/ml in three environments: 10 mM phosphate buffer, pH 7.3; 50% trifluoroethanol (TFE) in water; and in liposomes of 1-palmitoyl-2-oleoyl-*sn*-glycero-3-phosphocholine (POPC)/1-palmitoyl-2-oleoyl-*sn*-glycero-3-phosphoglycerol (POPG) (7:3 w/w, 2 mM), made as described above under fluorescence spectroscopy. In all cases, the peptide spectra were obtained by subtracting the spectra of the solution components in the absence of peptide.

2.6. Minimal inhibitory/haemolytic concentration

The peptide MICs, for the microorganisms listed in Section 2.1, were determined using the modified broth microdilution method in Muller Hinton (MH) medium [15]. The MIC was taken as the lowest peptide concentration at which no growth was observed after an overnight

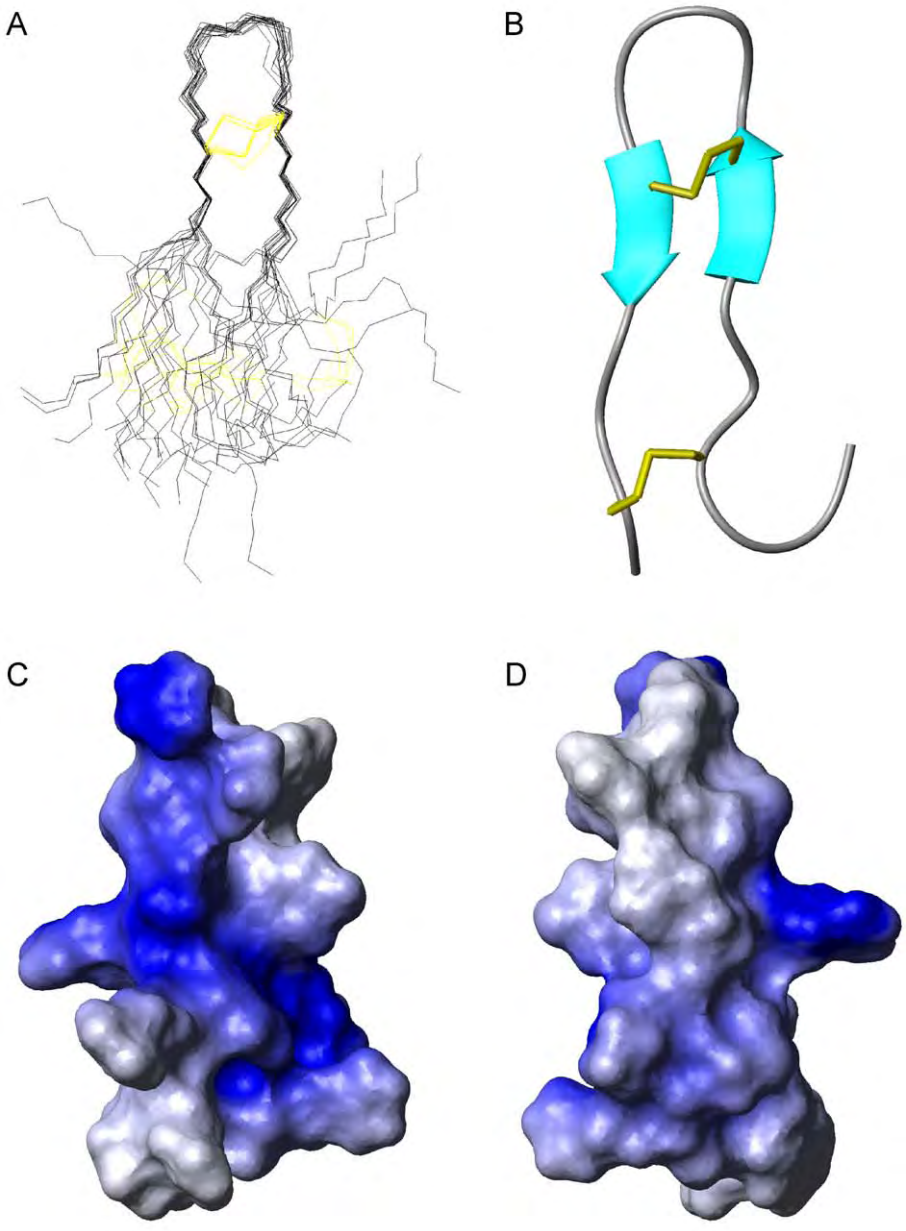

Fig. 4. Three-dimensional solution structure of polyphemusin I (PM1). (A) The set of 17 structures calculated for PM1. The backbone atoms are coloured black and the cysteine side chains are indicated in yellow. Structures are aligned over the β-sheet residues 7, 8, 13 and 14. (B) Ribbon diagram of a representative PM1 structure. (C) Contact surface painted with the electrostatic potential of a representative PM1 structure. (D) 180° rotation of the structure presented in panel C. In panels B, C, and D, the structure with the lowest average pairwise RMSD to the mean was selected as the representative. Figures were prepared with MOLMOL [35].

incubation at 37 °C. The minimal haemolytic concentration (MHC) was determined as previously described [36]. Briefly, human erythrocytes were collected in the presence of heparin, centrifuged to remove the buffy coat and washed three times in 0.85% saline. Serial dilutions of peptide in 0.85% saline were prepared and incubated with the erythrocytes for 4 h at 37 °C with constant nutating. The MHC was recorded as the concentration of peptide resulting in lysis. Both the MIC and MHC assays were performed three separate times and the mode values recorded.

2.7. Membrane depolarization assay

The cytoplasmic membrane depolarization activity of the peptides was determined as previously described [15] using *E. coli* strain DC2 and the membrane potential-sensitive dye, diSC$_3$5. The bacterial cells were collected in mid-log phase, washed in 5 mM HEPES buffer, pH 7.8, and resuspended in this buffer to an OD_{600} of 0.05. A diSC$_3$5 stock solution was added to a final concentration of 0.4 μM and the cell suspension was nutated at room temperature for 30 min. After this time, KCl was added to a final concentration of 100 mM and the suspension was incubated at room temperature for 10 min. A 2 ml cell suspension was placed in a 1 cm cuvette and a concentration of peptide was added. Changes in fluorescence were recorded with a model LS50B luminescence spectrometer (Perkin Elmer) at an excitation wavelength of 622 nm and an emission wavelength of 670 nm.

2.8. Fluorescence spectroscopy

Tryptophan fluorescence was recorded using a model LS50B luminescence spectrometer (Perkin Elmer) at an excitation wavelength of 280 nm and an emission range of 300–400 nm. Liposomes were prepared by dissolving POPC and POPG in chloroform at a ratio of 7:3 (w/w). The chloroform was removed under nitrogen and the lipids were dried under vacuum for 2 h and then suspended in 10 mM phosphate buffer (pH 7.3). Unilamellar vesicles were prepared by freeze–thawing the lipid solution five times (liquid N_2–air) followed by extrusion through two stacked 0.1 mm polycarbonate membranes (AMD Manufacturing, Inc.) which was repeated 10 times. Samples were run both in the presence or absence of 0.3 mM liposomes and a peptide concentration of 3 μg/ml. A spectrum of liposomes alone was subtracted to obtain the spectra due to peptide only.

2.9. Peptide translocation

The ability of peptides to translocate across model membranes was assayed as previously described [37]. Briefly, lipids (POPC/POPG/DNS-PE, 50:45:5) were dissolved in chloroform which was removed under a stream of N_2 and further dried under vacuum for 2 h. The lipid mixture was resuspended in a solution of 200 μM α-chymotrypsin in 150 mM NaCl, 20 mM HEPES buffer, pH 7.5. Unilamellar vesicles were prepared as described above under Section 2.8. Trypsin/chymotrypsin inhibitor was then added to inactivate the protease present outside the vesicles. Peptide was added at a concentration of 10 μg/ml and fluorescence transfer from the tryptophan residue in the peptide to the dansyl-group in DNS-PE was monitored for 500 s using a model LS50B luminescence spectrometer (Perkin Elmer) at an excitation wavelength of 280 nm and an emission wavelength of 510 nm. This assay was repeated three separate times and a representative trial is shown.

3. Results

3.1. NMR spectroscopy

Two-dimensional TOCSY, NOESY and DQF-COSY spectra were collected for both PM1 and PM1-S at 27 °C and pH 4.0. The PM1 and PM1-S proton resonances were assigned sequentially and the chemical shift assignments for PM1 are recorded in the supplementary information (Table S1). A region of the TOCSY spectrum is shown as Fig. 2A indicating the well-resolved spin systems in which there was no overlap of residues. The α-amide region of the NOESY spectrum is shown as Fig. 2B, indicating the sequentially assigned backbone proton resonances. Some degree of overlap was observed with the α-proton resonances in the F1 axis however, due to good separation of amide resonances in the F2 axis, this did not pose a problem in the assignment of crosspeaks. Strong $d_{\alpha N}(i,i+1)$ contacts were observed throughout the molecule and are typical of β-sheet structure while strong $d_{NN}(i,i+1)$ contacts observed between residues 10 and 12 are characteristic of a β-turn [38]. In addition, several long-range contacts, separated by as many as 15 residues, were further evidence of the disulfide-constrained anti-parallel β-hairpin structure that

Table 1
Structural statistics of 17 polyphemusin I (PM1) structures determined by Xplor-NIH

NOE Restraints	
Total	143
Intra-residue	69
Inter-residue	74
Restraint violations (mean number per structure)	
>0.1 Å	0.47 ± 0.62
Mean final energy (kcal mol^{-1})	
E_{Total}	22.8 ± 1.1

Mean pairwise RMSD		
Alignment	Backbone	Heavy
Turn (8–13)	0.24 ± 0.15	1.20 ± 0.35
Sheet (7, 8, 13, 14)	0.22 ± 0.10	0.86 ± 0.36

is polyphemusin I. A figure indicating the observed inter-residue NOE contacts is provided in the supplementary information.

3.2. NOE data analysis and structure calculation

The structure of polyphemusin I was calculated using 143 total NOE restraints (69 intra-residue and 74 inter-residue restraints). Fig. 3 indicates the distribution of inter-residue restraints, which were spread evenly throughout the molecule rather than originating from a few select residues. With the exception of arginines 6 and 10, the number of inter-residue restraints was greater than or equal to the number of intra-residue restraints for all residues. The set of 17 calculated polyphemusin I structures is presented as Fig. 4A. Rather than calculate an average structure, a schematic diagram of the conformer with the lowest average pairwise RMSD to the mean is shown as Fig. 4B. The structure of polyphemusin I was that of an anti-parallel β-hairpin connected by a type I′ β-turn [39]. The structure was well-defined in the β-sheet region (residues 7, 8, 13, 14) with an average pairwise RMSD of 0.22 ± 0.10 and 0.86 ± 0.36 Å for backbone and heavy atoms, respectively (Table 1). The sheet region was variable throughout the calculated structures but, based upon Procheck analysis [33,34], might extend from residues 4 to 9 and residues 12 to 17 (data not shown). Fig. 4C and D show the contact surface of the molecule painted with the electrostatic potential of the representative PM1 structure. From the hydrophilic face of the molecule shown in panel C, a cationic cleft was observed, running the length of the molecule and wrapping around the surface in a diagonal fashion. A

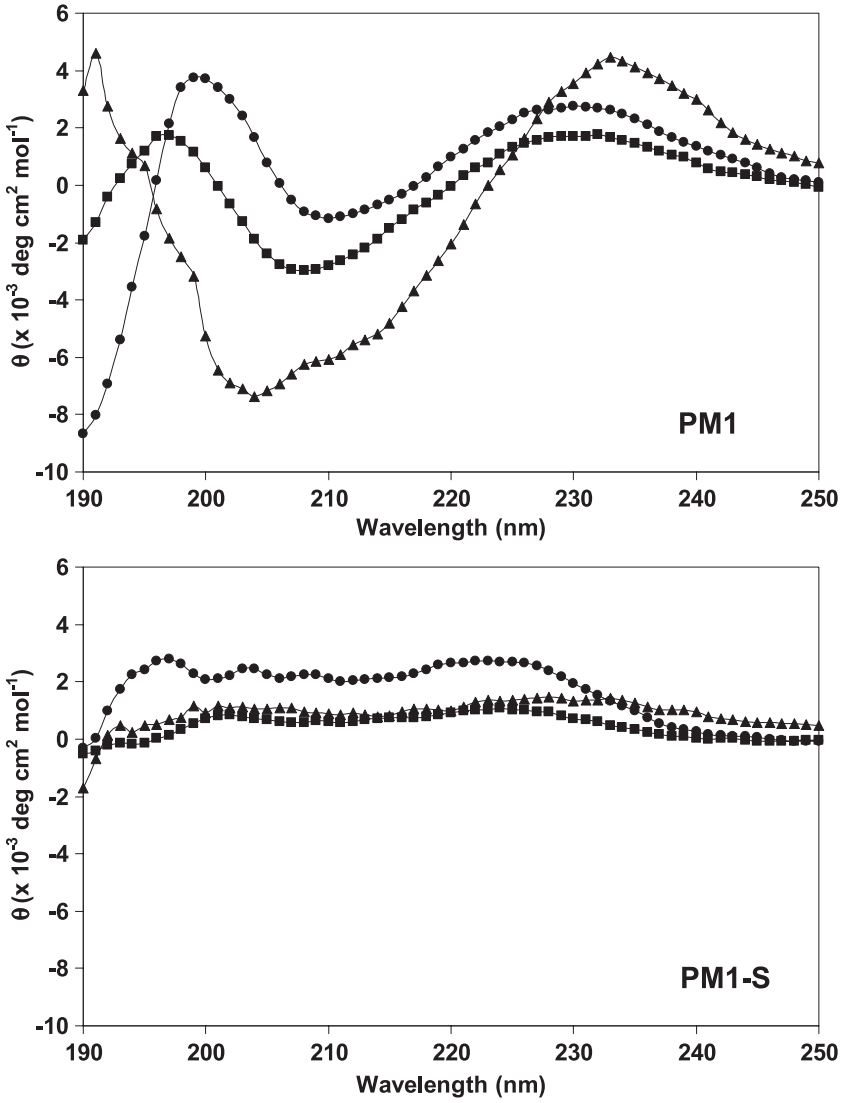

Fig. 5. CD spectra of polyphemusin I (PM1) and PM1-S. Spectra were recorded in 10 mM phosphate buffer, pH 7.3 (circles); 50% TFE in H_2O (squares); and liposomes of POPC/POPG (7:3 w/w, 2 mM) (triangles). Peptide concentration was 100 μg/ml.

180° rotation of this structure revealed the more hydrophobic face of the molecule and is shown as panel D.

Detailed analysis of the NOESY spectrum of PM1-S yielded 97 unambiguous restraints (58 intra-residue, 39 inter-residue) that were used in structure calculation (data not shown). Of the 39 inter-residue restraints the majority were short range (i, i + 1) and only two could be classified as medium range (i, i + 2 and i, i + 3). This led to the generation of a large number of low-energy structures with no distinct population displaying a preferred conformation (data not shown).

3.3. Circular dichroism spectroscopy

The CD spectra of PM1 and PM1-S recorded in phosphate buffer, TFE, and in the presence of liposomes are shown in Fig. 5. The spectrum of PM1 in buffer displayed two positive bands at 200 and 230 nm and one negative band at 210 nm. These bands are indicative of a β-sheet structure and a β-turn [40] and this spectra is very similar to that of the related peptide tachyplesin I [16]. The spectrum of PM1 in TFE displayed a similar pattern with one of the positive bands shifted slightly to 196 nm and the negative band shifted to 208 nm. These shifts were due to the presence of TFE, which is capable of stabilizing protein conformations that would be unordered in aqueous environments [16], thus producing a spectrum that is more similar to that in liposomes than in aqueous buffer. The PM1 spectrum in the anionic liposome environment displayed a positive band below 197 and at 234 nm and a negative band at 204 nm, again indicating the presence of a β-sheet structure and a β-turn. The slight differences in wavelength of the bands are likely to be due to the environment in which the peptide was located and the stabilizing forces imparted by that environment. As the environment decreased in polarity, protein secondary structures, particularly those in small peptides, become stabilized due to decreased interference of hydrogen bonding with surrounding polar molecules (buffer).

The CD spectra of PM1-S indicated that, in all environments, the peptide displayed no observable patterns that could be related to structural features. This indicates that PM1-S is a flexible molecule with no favoured conformation.

3.4. Minimal inhibitory concentration

The MICs of peptides PM1 and PM1-S against a variety of microorganisms are shown in Table 2. PM1 showed high antimicrobial activity against the Gram-negative, Gram-positive and fungal specimens tested with MICs ranging from 0.5 to 4 μg/ml. The linear peptide, PM1-S, was not as active as the native peptide, possessing a wide range of MICs from 2 to 64 μg/ml. In addition, PM1-S remained active against Gram-negative bacteria but displayed poor activity to both Gram-positive and fungal microorganisms. Overall, PM1-S was 4- to 16-fold less active than the parent, PM1.

Table 2
Antimicrobial and haemolytic activity of PM1 and PM1-S

Strains	MIC/MHC (μg/ml)	
	PM1	PM1-S
Gram-negative		
E. coli UB1005	0.5	4
E. coli DC2	1	4
S. typhimurium (defensin-sensitive)	0.25	2
S. typhimurium	1	8
P. aeruginosa K799	2	32
P. aeruginosa Z61	1	16
Gram-positive		
S. aureus SAP0017	2	32
S. epidermidis	1	16
E. faecalis	1	2
C. albicans	4	64
Human erythrocytes	>64	>256

3.5. Membrane depolarization

To assess bacterial membrane depolarization, the membrane potential-sensitive dye diSC$_3$5 was used. This cationic dye concentrates in the cytoplasmic membrane under the influence of the membrane potential (which is oriented internal negative) resulting in a self-quenching of fluorescence. Upon disruption of the membrane potential, the dye dissociates into the buffer leading to an increase in fluorescence [8]. Depolarization was monitored over a period of 800 s for PM1 and PM1-S (Fig. 6). The ability of PM1 to depolarize bacterial cells was much greater than that of PM1-S with the lowest concentration of PM1, 1 μg/ml, producing the same fluorescence increase as the maximum utilized concentration of PM1-S, 5 μg/ml. Overall, PM1-S displayed a 2- to 4-fold reduction in its ability to depolarize the bacterial cytoplasmic membrane when compared to PM1. In addition, PM1 was fast acting, achieving maximum fluorescence at 400 s. In contrast, the lag time of PM1-S was much longer, leading to maximum fluorescence being achieved after 600 s.

3.6. Fluorescence spectroscopy

To determine the local environment of the peptides, the fluorescence emission of the single tryptophan residue was monitored. Tryptophan fluorescence is a widely used method to determine the polarity of the local environment, as it is a natural fluorophore in proteins. In a polar environment, excited fluorophores interact with polar solvent molecules decreasing the energy of the excited state [41]. This decrease in energy is observed as a reduction of fluorescence intensity and an increase in fluorescence wavelength. As the polarity of the environment decreases, tryptophan fluorescence occurs at a decreased wavelength (a blue shift) with an increase in intensity. The tryptophan

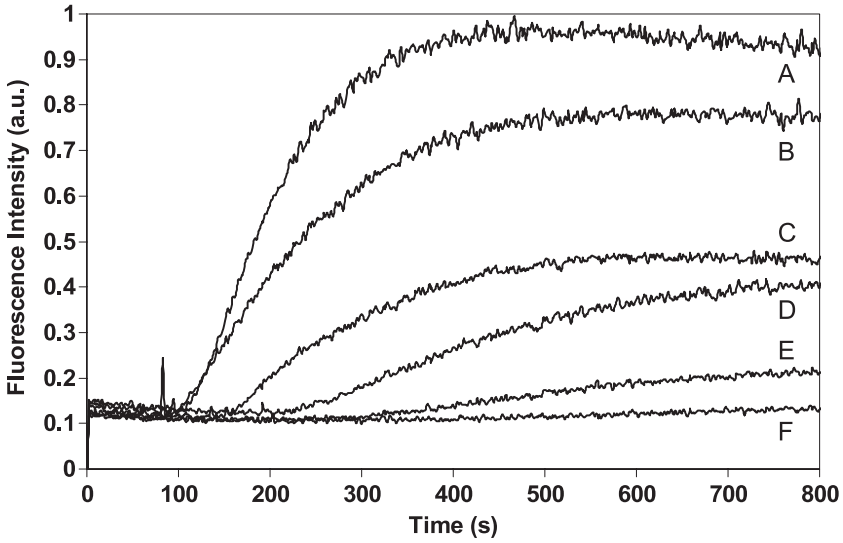

Fig. 6. Cytoplasmic membrane depolarization of *E. coli* DC2 by polyphemusin I (PM1) and PM1-S using the membrane potential-sensitive dye, $diSC_3 5$. Dye release was monitored at an excitation wavelength of 622 nm and an emission wavelength of 670 nm. In each run, peptide was added near the 100 s mark. PM1: (A) 5 μg/ml; (B) 3 μg/ml; (C) 1 μg/ml. PM1-S: (D) 5 μg/ml; (E) 3 μg/ml; (F) 1 μg/ml.

fluorescence spectra for PM1 and PM1-S are shown in Fig. 7. Both PM1 and PM1-S displayed similar blue shifts of −10.1 and −8.37 nm, respectively, when present in a hydrophobic lipid environment compared to a hydrophilic aqueous environment. The fluorescence intensities of PM1 and PM1-S were also found to increase 6-fold and 5-fold, respectively, in a liposome solution compared to buffer. These findings indicate that both peptides were able to associate with and insert their tryptophan side chains into the lipid bilayer of the model membrane.

3.7. Peptide translocation

The ability of the peptides to translocate model membranes was assayed using a system that was previously described in detail [42]. As the peptides gain access to the internal cavity of the liposome they are digested by protease leading to a reduction in observed fluorescence transfer. The fluorescence spectra of both peptides recorded over a period of 500 s are shown in Fig. 8. The ability of PM1 to translocate the model membrane

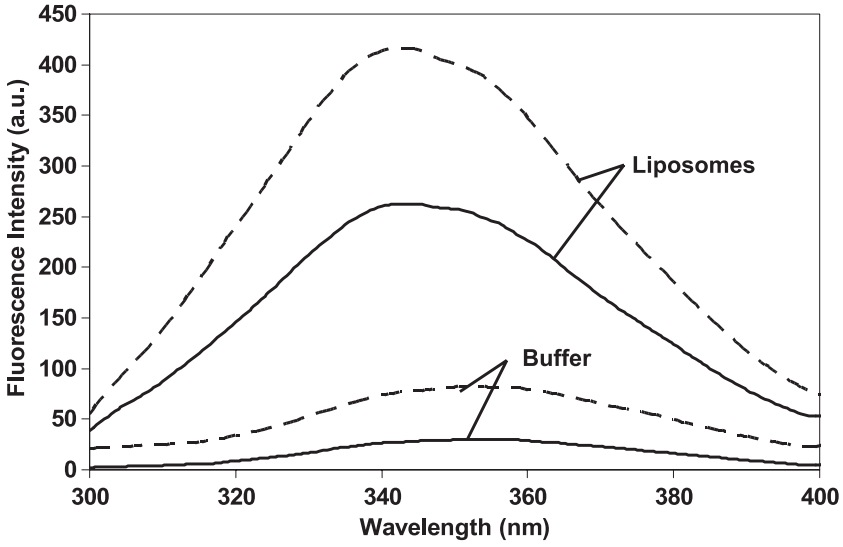

Fig. 7. Fluorescence spectra of polyphemusin I (PM1) and PM1-S in aqueous solution and in the presence of liposomes. Samples contained 3 μg/ml peptide in 10 mM phosphate buffer, pH 7.3, and 0.3 mM POPC/POPG (7:3 w/w) liposomes. Excitation wavelength was 280 nm. Solid and dotted lines indicate PM1 and PM1-S, respectively.

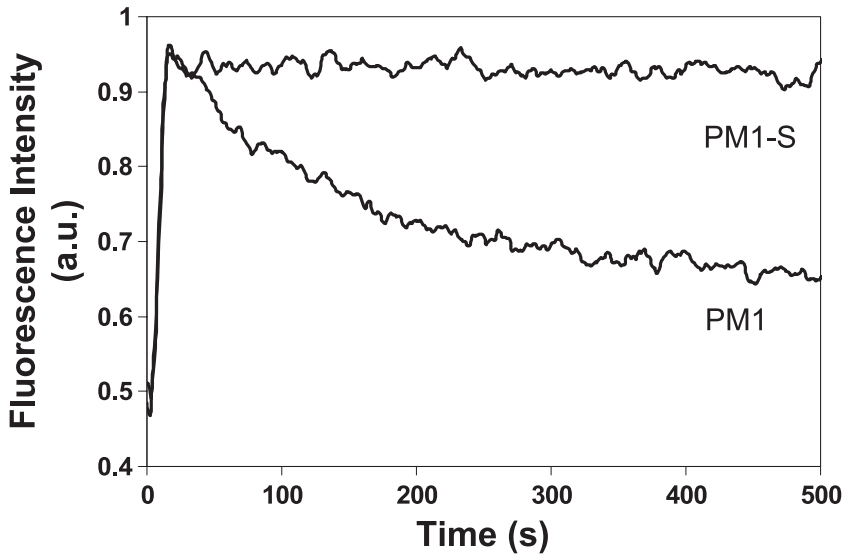

Fig. 8. Membrane translocation of polyphemusin I (PM1) and PM1-S as measured by fluorescence transfer from tryptophan to DNS-PE. A decrease in fluorescence transfer, due to proteolytic degradation of the peptide by internalized α-chymotrypsin, is used as measure of membrane translocation. The lipid concentration was 200 μM and the peptide concentration was 10 μg/ml. Fluorescence transfer was monitored at an excitation wavelength of 280 nm and an emission wavelength of 510 nm.

system was indicated by the steady decrease in fluorescence, beginning almost immediately after addition of the peptide. This finding is in agreement with previously published translocation data for PM1 [42]. In contrast, no decrease in fluorescence was observed in the spectra of PM1-S throughout the 500 s, indicating a complete lack of membrane translocation.

4. Discussion

To examine the effects of conformational flexibility and disulfide-constrained rigidity upon the antimicrobial peptide polyphemusin I, a cysteine-substituted analogue was created. This analogue, PM1-S, was synthesized with all four cysteine residues simultaneously substituted with serine. Serine was chosen, as its side chain is similar to that of cysteine in structure, polarity and hydrogen bonding ability.

Due to sequence similarity, the structure of polyphemusin I has been assumed to be similar to the NMR structures of the related peptides tachyplesin I, and the polyphemusin variant T22, and indeed only subtle differences were observed here. We determined the three-dimensional solution structure of polyphemusin I by ^{1}H-NMR and an ensemble of the 17 lowest energy structures is presented here (Fig. 3). The structure of PM1 is that of an antiparallel β-hairpin. The amphipathic nature of the molecule is more clearly defined than previously modelled [43] and a cationic cleft can be observed running the length of the molecule. The high affinity of polyphemusin I for LPS has been determined previously [42] and this cleft may represent the binding site for the negatively charged phosphate groups present on the LPS molecule. The structure of PM1 is well-defined throughout the sheet and loop regions but is quite flexible in the tail portion. Structural studies of tachyplesin I have previously a central ‘‘hinge’’ region in the molecule which, in a membrane environment, allows the molecule to fold in a manner with an increased hydrophobic surface [17]. The flexible region of polyphemusin I may flank an analogous hinge and this would be expected to play a role in LPS binding, peptide translocation and antimicrobial activity.

NMR spectroscopy was also used in an attempt to determine the structure of the linear peptide, PM1-S. Analysis of the NOESY spectrum revealed 97 NOEs (58 intra-residue and 39 inter-residue), of which only two could be classified as medium range (one i,i + 2, and one i,i + 3), and no long-range NOEs were observed. From these findings it was concluded that PM1-S is unstructured in solution and further analysis by CD spectroscopy indicated that the peptide remained unstructured in both 50% TFE and POPC/POPG liposome environments.

Both PM1 and PM1-S displayed antimicrobial properties with the linear peptide being 2- to 16-fold less active. Linearizing the peptide had a marginally lesser effect against Gram-negative than Gram-positive bacteria. We presume this reflects the fact that the linear peptide is better able to access the self-promoted uptake pathway, where the initial interacting molecule is lipopolysaccharide. Thus translocation across the outer membrane would be less affected than translocation across the cytoplasmic membrane (which reflects differential translocation as assessed by the liposome translocation assay). Comparing the activity of PM1-S to previously characterized extended and helical peptides [42,44], it should be noted that the linear peptide retains

considerable activity when compared to the excellent MICs of polyphemusin I, despite its lack of structure.

In an effort to account for this reduction in activity, a variety of membrane interaction assays were performed. The ability of both peptides to depolarize membranes was assayed using the membrane potential-sensitive dye $diSC_35$ and the *E. coli* DC2 strain. The linear peptide PM1-S displayed a 4-fold reduction in membrane depolarization, which correlated with the observed reduction in antimicrobial activity. In addition, PM1-S displayed a much longer lag time in reaching maximum fluorescence, suggesting a possible decrease in the rate of membrane association when compared to PM1. A tryptophan fluorescence assay indicated that both peptides were able to associate with model membranes, thus, membrane association per se did not account for differences in activity.

Since polyphemusin I has previously been shown to translocate model membranes and is thought to exert its antimicrobial actions from within the cell [42], a translocation assay was performed in an attempt to explain the reduction in PM1-S activity. It was found that, while PM1 is an effective translocator, PM1-S appeared incapable of translocating model membranes. Thus, it appeared that linear peptide acts through a different mechanism of antimicrobial activity than polyphemusin I as the inability of PM1-S to translocate membranes might be expected to lead to a complete loss of activity rather than a 4- to 16-fold reduction. Indeed PM1-S may be acting on membranes in a manner consistent with the aggregate model [5] of antimicrobial activity in which structure is not a requirement for function. This is further supported by the ability of PM1-S to bind membranes and depolarize bacterial cells, two outcomes that would be expected from a peptide functioning through such a mechanism.

The data presented here indicate that the disulfide-constrained, β-sheet structure of polyphemusin I is required for maximal antimicrobial activity. Interruption of this β-sheet structure results in a peptide with measurable, albeit reduced, activity and completely abolishes the ability of the peptide to translocate membranes. The lack of preferred conformation and inability to translocate membranes combined with the moderate antimicrobial activity of PM1-S indicates that the linear peptide is acting through a different mechanism than polyphemusin I. In addition, the new availability of the polyphemusin I solution structure makes it possible to conduct future structure–activity studies on this highly active antimicrobial peptide.

Acknowledgements

We acknowledge funding from the Canadian Bacterial Diseases Network to REWH. REWH is the recipient of a Canada Research Chair and JPSP is the recipient of an NSERC Industrial Postgraduate Scholarship kindly supported by Helix BioMedix, Inc. The authors would like to thank Dr. Mark Okon for acquisition of the NMR spectra and Mrs. Suzanne Perry-Riehm for acquisition of the mass spectra as well as Dr. Lijuan Zhang, David Jung, Dr. Danika Goosney and Joseph McPhee for critical help in preparing this paper.

References

[1] T. Miyata, F. Tokunaga, T. Yoneya, K. Yoshikawa, S. Iwanaga, M. Niwa, T. Takao, Y. Shimonishi, Antimicrobial peptides, isolated from horseshoe crab hemocytes, tachyplesin II, and polyphemusins I and II: chemical structures and biological activity, J. Biochem. (Tokyo) 106 (1989) 663–668.

[2] T. Nakamura, H. Furunaka, T. Miyata, F. Tokunaga, T. Muta, S. Iwanaga, M. Niwa, T. Takao, Y. Shimonishi, Tachyplesin, a class of antimicrobial peptide from the hemocytes of the horseshoe crab (*Tachypleus tridentatus*). Isolation and chemical structure, J. Biol. Chem. 263 (1988) 16709–16713.

[3] H. Tamamura, M. Kuroda, M. Masuda, A. Otaka, S. Funakoshi, H. Nakashima, N. Yamamoto, M. Waki, A. Matsumoto, J.M. Lancelin, et al., A comparative study of the solution structures of tachyplesin I and a novel anti-HIV synthetic peptide, T22 ([Tyr5,12, Lys7]-polyphemusin II), determined by nuclear magnetic resonance, Biochim. Biophys. Acta 1163 (1993) 209–216.

[4] K. Kawano, T. Yoneya, T. Miyata, K. Yoshikawa, F. Tokunaga, Y. Terada, S. Iwanaga, Antimicrobial peptide, tachyplesin I, isolated from hemocytes of the horseshoe crab (*Tachypleus tridentatus*). NMR determination of the beta-sheet structure, J. Biol. Chem. 265 (1990) 15365–15367.

[5] D. Andreu, L. Rivas, Animal antimicrobial peptides: an overview, Biopolymers 47 (1998) 415–433.

[6] R.E.W. Hancock, A. Rozek, Role of membranes in the activities of antimicrobial cationic peptides, FEMS Microbiol. Lett. 206 (2002) 143–149.

[7] H.G. Boman, B. Agerberth, A. Boman, Mechanisms of action on *Escherichia coli* of cecropin P1 and PR-39, two antibacterial peptides from pig intestine, Infect. Immun. 61 (1993) 2978–2984.

[8] M. Wu, E. Maier, R. Benz, R.E.W. Hancock, Mechanism of interaction of different classes of cationic antimicrobial peptides with planar bilayers and with the cytoplasmic membrane of *Escherichia coli*, Biochemistry 38 (1999) 7235–7242.

[9] C.B. Park, H.S. Kim, S.C. Kim, Mechanism of action of the antimicrobial peptide buforin II: buforin II kills microorganisms by penetrating the cell membrane and inhibiting cellular functions, Biochem. Biophys. Res. Commun. 244 (1998) 253–257.

[10] A. Yonezawa, J. Kuwahara, N. Fujii, Y. Sugiura, Binding of tachyplesin I to DNA revealed by footprinting analysis: significant contribution of secondary structure to DNA binding and implication for biological action, Biochemistry 31 (1992) 2998–3004.

[11] R.I. Lehrer, A. Barton, K.A. Daher, S.S. Harwig, T. Ganz, M.E. Selsted, Interaction of human defensins with *Escherichia coli*. Mechanism of bactericidal activity, J. Clin. Invest. 84 (1989) 553–561.

[12] A. Patrzykat, C.L. Friedrich, L. Zhang, V. Mendoza, R.E.W. Hancock, Sublethal concentrations of pleurocidin-derived antimicrobial peptides inhibit macromolecular synthesis in *Escherichia coli*, Antimicrob. Agents Chemother. 46 (2002) 605–614.

[13] M. Mandal, R. Nagaraj, Antibacterial activities and conformations of synthetic alpha-defensin HNP-1 and analogs with one, two and three disulfide bridges, J. Pept. Res. 59 (2002) 95–104.

[14] Z. Wu, D.M. Hoover, D. Yang, C. Boulegue, F. Santamaria, J.J. Oppenheim, J. Lubkowski, W. Lu, Engineering disulfide bridges to dissect antimicrobial and chemotactic activities of human beta-defensin 3, Proc. Natl. Acad. Sci. U. S. A. 100 (2003) 8880–8885.

[15] M. Wu, R.E.W. Hancock, Interaction of the cyclic antimicrobial cat-

ionic peptide bactenecin with the outer and cytoplasmic membrane, J. Biol. Chem. 274 (1999) 29–35.
[16] A.G. Rao, Conformation and antimicrobial activity of linear derivatives of tachyplesin lacking disulfide bonds, Arch. Biochem. Biophys. 361 (1999) 127–134.
[17] A. Laederach, A.H. Andreotti, D.B. Fulton, Solution and micelle-bound structures of tachyplesin I and its active aromatic linear derivatives, Biochemistry 41 (2002) 12359–12368.
[18] D. Clark, Novel antibiotic hypersensitive mutants of *Escherichia coli* genetic mapping and chemical characterization, FEMS Microbiol. Lett. 21 (1984) 189–195.
[19] P.I. Fields, E.A. Groisman, F. Heffron, A Salmonella locus that controls resistance to microbicidal proteins from phagocytic cells, Science 243 (1989) 1059–1062.
[20] B.L. Angus, A.M. Carey, D.A. Caron, A.M. Kropinski, R.E.W. Hancock, Outer membrane permeability in *Pseudomonas aeruginosa*: comparison of a wild-type with an antibiotic-supersusceptible mutant, Antimicrob. Agents Chemother. 21 (1982) 299–309.
[21] J. Tam, C. Wu, W. Liu, J. Zhang, Disulfide bond formation in peptides by dimethyl sulfoxide. Scope and applications, J. Am. Chem. Soc. 113 (1991) 6657–6662.
[22] M. Rance, O.W. Sorensen, G. Bodenhausen, G. Wagner, R.R. Ernst, K. Wuthrich, Improved spectral resolution in COSY ^{1}H-NMR spectra of proteins via double quantum filtering, Biochem. Biophys. Res. Commun. 117 (1983) 479–485.
[23] L. Braunschweiler, R.R. Ernst, Coherence transfer by isotropic mixing: application to proton correlation spectroscopy, J. Magn. Res. 53 (1983) 521–528.
[24] J. Jeener, B.H. Meier, P. Bachmann, R.R. Ernst, Investigation of exchange processes by two-dimensional NMR spectroscopy, J. Chem. Phys. 71 (1979) 4546–4553.
[25] M. Piotto, V. Saudek, V. Sklenar, Gradient-tailored excitation for single-quantum NMR spectroscopy of aqueous solutions, J. Biomol. NMR 2 (1992) 661–665.
[26] V. Sklenar, M. Piotto, R. Leppik, V. Saudek, Gradient-tailored water suppression for 1H–15N HSQC experiments optimized to retain full sensitivity, J. Magn. Reson., Ser. A 102 (1993) 241–245.
[27] A. Bax, D.G. Davis, MLEV-17 based two-dimensional homonuclear magnetization transfer spectroscopy, J. Magn. Res. 65 (1985) 355–360.
[28] F. Delaglio, S. Grzesiek, G.W. Vuister, G. Zhu, J. Pfeifer, A. Bax, NMRPipe: a multidimensional spectral processing system based on UNIX pipes, J. Biomol. NMR 6 (1995) 277–293.
[29] B.A. Johnson, R.A. Blevins, NMRView: a computer program for the visualization and analysis of NMR data, J. Biomol. NMR 4 (1994) 603–614.
[30] S.G. Hyberts, M.S. Goldberg, T.F. Havel, G. Wagner, The solution structure of eglin c based on measurements of many NOEs and coupling constants and its comparison with X-ray structures, Protein Sci. 1 (1992) 736–751.
[31] C.L. Friedrich, A. Rozek, A. Patrzykat, R.E.W. Hancock, Structure and mechanism of action of an indolicidin peptide derivative with improved activity against gram-positive bacteria, J. Biol. Chem. 276 (2001) 24015–24022.
[32] C.D. Schwieters, J.J. Kuszewski, N. Tjandra, G.M. Clore, The Xplor-NIH NMR molecular structure determination package, J. Magn. Res. 160 (2003) 66–74.
[33] A.L. Morris, M.W. MacArthur, E.G. Hutchinson, J.M. Thornton, Stereochemical quality of protein structure coordinates, Proteins 12 (1992) 345–364.
[34] R.A. Laskowski, M.W. MacArthur, D.S. Moss, J.M. Thornton, PROCHECK: a program to check the stereochemical quality of protein structures, J. Appl. Crystallogr. 26 (1993) 283–291.
[35] R. Koradi, M. Billeter, K. Wuthrich, MOLMOL: a program for display and analysis of macromolecular structures, J. Mol. Graph 14 (1996) 51–55, 29–32.
[36] L. Zhang, R. Benz, R.E.W. Hancock, Influence of proline residues on the antibacterial and synergistic activities of alpha-helical peptides, Biochemistry 38 (1999) 8102–8111.
[37] S. Kobayashi, K. Takeshima, C.B. Park, S.C. Kim, K. Matsuzaki, Interactions of the novel antimicrobial peptide buforin 2 with lipid bilayers: proline as a translocation promoting factor, Biochemistry 39 (2000) 8648–8654.
[38] K. Wuthrich, NMR of Proteins and Nucleic Acids, Wiley, Toronto, 1986.
[39] J.S. Richardson, The anatomy and taxonomy of protein structure, Adv. Protein Chem. 34 (1981) 167–339.
[40] G.D. Fasman, Circular Dichroism and the Conformational Analysis of Biomolecules, Plenum, New York, 1996.
[41] I.D. Campbell, R.A. Dwek, Biological Spectroscopy, The Benjamin/Cummings Publishing, Menlo Park, 1984.
[42] L. Zhang, A. Rozek, R.E.W. Hancock, Interaction of cationic antimicrobial peptides with model membranes, J. Biol. Chem. 276 (2001) 35714–35722.
[43] L. Zhang, M.G. Scott, H. Yan, L.D. Mayer, R.E.W. Hancock, Interaction of polyphemusin I and structural analogs with bacterial membranes, lipopolysaccharide, and lipid monolayers, Biochemistry 39 (2000) 14504–14514.
[44] T.J. Falla, D.N. Karunaratne, R.E.W. Hancock, Mode of action of the antimicrobial peptide indolicidin, J. Biol. Chem. 271 (1996) 19298–19303.